ORIGINAL PAPER

Theoretical study of geometrical and nonlinear optical properties of pyridinum *N*-phenolate betaine dyes

Wawrzyniec Niewodniczański · Wojciech Bartkowiak

Abstract This paper presents an ab initio quantum chemical investigation of the geometrical structures and the nonlinear optical properties (NLO) of three structural isomers of pyridinium *N*-phenolate betaine dye. The ground state geometrical parameters and the first-order hyperpolarizabilities were calculated using the Hartree-Fock (HF) as well as the second-order perturbation Møller-Pleset (MP2) method with the 6–31G, 6–31G(d), 6–31G(d,p), 6–31+G(d), 6–31++G(d,p), 6–311+G(d), aug-cc-PVDZ and the recently developed Z3PolX basis sets. Moreover, the first-order hyperpolarizability was calculated at the coupled cluster singles and doubles (CCSD/6–31+G(d)) level of theory. The analysis of the results of calculations for the investigated isomers indicates that there are important differences in their NLO activities. Additionally, it was shown that Z3PolX basis set works reasonable well for betaine dyes.

Keywords Basis set effect · Betaine dyes · Electron correlation · Non-linear optical properties · Torsional barrier

Introduction

Most of molecular materials used nowadays in the nonlinear optics are ferromagnetic non-organic crystals, but they have significant disadvantages (in the first place,

W. Niewodniczański (✉) · W. Bartkowiak
Institute of Physical and Theoretical Chemistry,
Wroclaw University of Technology,
Wybrzeże Wyspiańskiego 27,
Wrocław, Poland
e-mail: wawrzyniec.niewodniczanski@pwr.wroc.pl

W. Bartkowiak
e-mail: wojciech.bartkowiak@pwr.wroc.pl

relatively slow optical switching time) [1, 2]. Therefore, organic materials attract a great level of attention [2–4]. Conventional organic molecules used for the non-linear optics consist of an electron donor and acceptor substituents connected by a π-electron system [3]. However, chemists continuously work to design other molecules exhibiting large non-linear optical (NLO) response. Paley and Harris, using the two-state model [5], suggested that pyridinium *N*-phenolate betaine dyes, famous for theirs large negative solvatochromism [6–9], should have large NLO response [10, 11]. They pointed out that the same properties which are the reason of such a remarkable solvatochromism, large dipole moment difference between ground and low-laying charge transfer (CT) excited state, cause the large first-order hyperpolarizability (β). Abe et al. went a step further and described a new approach in the molecular design of the NLO materials, through the use of the heterocyclic betaine dyes [12, 13]. In betaine dyes electrodonating (D) and electrowithdrawing (A) groups are directly linked and the charge transfer has the short range character. Abe et al. also described the way of modifying the betaines to enlarge NLO response and create molecules easier to prepare as a bulk material [14, 15]. Laxmikanth Rao et al. classified the betaine dyes as molecules with π-electron system separated by σ type bond and suggested that this group of molecules shows potential application in NLO materials [16, 17]. Finally, it was found that the electron structure of the heterocyclic betaine dyes strongly depends on conformational parameters [18–25]. For example, it has been shown that the first- and the second-order hyperpolarizability [19, 20, 23], as well as the two-photon absorption cross section [23] have maximum value near central interplanar angle (ϕ) equal to 80° (see Fig. 1).

The aim of the present study is to investigate differences and similarities between three pyridinium
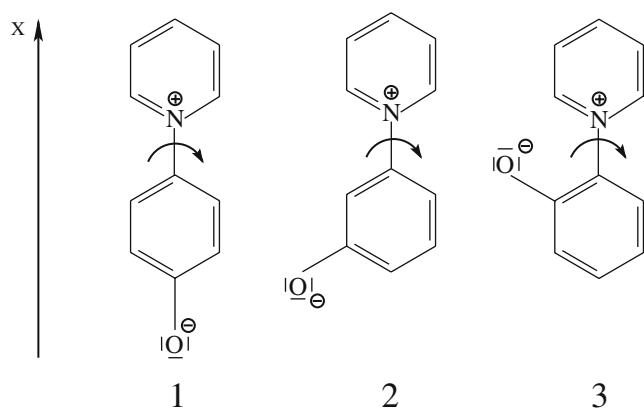
Fig. 1 Betaine dyes investigated in the present study

N-phenolate betaine dyes (Fig. 1). Most previous research were concentrated on 4-(1-pyridinium-1-yl)phenolate (**1**) molecule [16, 20, 22, 23, 26–34], the smallest derivative of the well-known Reichardt's betaine dye. There are also a few studies of its *ortho* isomer (**3**) [25, 32, 35]. Surprisingly, there have been no literature reports about either isomer with oxygen in *meta* position (**2**), or any of its derivatives.

One of the most interesting findings of our previous study is that the inclusion of dynamic electron correlation significantly changes the geometrical properties of the betaine **1** [33]. As a consequence the values of the first-order hyperpolarizability decrease after the inclusion of electron correlation [34], what is rather unusual behaviour for organic molecules [34, 36]. Therefore, the electron correlation effects on the geometry of the investigated molecules is analyzed. Another issue is how the inclusion of the electron correlation changes the value of the first-order hyperpolarizability of isomers **2** and **3**. Additionally, we would like to determine the dependence of the first-order hyperpolarizability on the interplanar angle (φ) as well as the dispersion effect of β for all three isomers.

Z3PolX basis set was design to perform electric dipole moment (μ) and polarizability (α) calculations of large molecular systems [37–39]. Recently, it was reported that the Z3PolX basis set also reproduce reasonable well the vibrational [40] and electronic [41] first-order hyperpolarizability of organic molecules. Therefore, final issue address in this study was to compare the β values obtained with Z3PolX basis set and the commonly used Pople's basis sets as well as Dunning's correlation consistent aug-cc-PVDZ basis set.

Computational details

Most of the calculations were performed using the GAUSSIAN03 program [42]. The calculations of the frequency dependent first-order hyperpolarizability were performed using the GAMESS package [43]. Moreover, the calculations of the static first-order hyperpolarizability at the coupled cluster singles and doubles (CCSD) level of theory were carried out with DALTON 2.0 program [44]. Default settings were used in all of the programs. The optimal geometries were obtained at the HF and MP2 levels of theory without any symmetry restrictions. The data presented in the previous paper indicated that the 6–31G(d) basis set had seemed to be a good compromise between an accuracy and a computational costs in the case of calculation of the geometrical parameters for the molecule **1** [33]. Therefore, this basis set was used in the present study in order to obtain optimal geometries of all isomers. The potential energy scan for the central torsional angle was obtained using the standard scan technique implemented in the GAUSSIAN program. It means that during the scan of energy the consecutive geometries were obtained by keeping fixed values of the angle φ ranging from 0° to 90°, while the remaining parameters were allowed to relax. Recently, the 6–31+G(d) basis set has been recommended for estimation of the NLO properties of medium-size molecules [45, 46]. Thus, in this study mainly the 6–31+G(d) basis set, together with recently developed medium-size polarized Z3PolX basis set and correlation consistent aug-cc-PVDZ basis set, was chosen to obtain the first-order hyperpolarizability. For comparison the following basis sets were also used: 6–31G, 6–31G(d), 6–31G(d,p), 6–31++G(d,p) and 6–311+G(d) for the molecule **1**. In this case, the tensor components of the static first-order hyperpolarizability (β_{ijk}) were calculated at the HF and MP2 levels of theory using the numerical differentiation method referred to as finite field (FF) technique [47]. The frequency dependent first-order hyperpolarizability [$\beta(-\omega_1, \omega_2, \omega_3)$] was obtained within the time dependent Hartree-Fock (TDHF) method using the 6–31+G(d) basis set. The values of β for the range of frequencies 0.0–0.03 a.u. were obtained from the following equation fitting of the calculated data [48]:

$$\beta(-\omega_\sigma, \omega_2, \omega_3) = \beta(0,0,0)\left[1 + A\omega_L^2 + B\omega_L^4\right], \qquad (1)$$

with $\omega_\sigma = \omega_1 + \omega_2$ and $\omega_L^2 = \omega_\sigma^2 + \omega_1^2 + \omega_2^2$. Additionally, values of β were obtained for two laser characteristic frequencies: 0.04282 a.u. (Nd:YAG laser wavelength — 1064 nm) and 0.06563 a.u. (694.3 nm for ruby laser). The following approximation (multiplicative correction) for the correlated dynamic properties was used to calculate the frequency dependent β at the MP2 level [49, 50]:

$$\beta^{MP2}(\omega) \approx \frac{\beta^{MP2}(0)}{\beta^{SCF}(0)}\beta^{SCF}(\omega) \qquad (2)$$

The calculated components of the β_{ijk} tensor were transformed to the vector component (experimentally available for polar molecules) defined as [3]:

$$\beta_\mu = \sum_i \frac{\beta_i \mu_i}{|\mu|} \qquad i \in (x,y,z) \qquad (3)$$

with

$$\beta_i = \frac{3}{5} \sum_i \beta_{ijj} \qquad j \in (x,y,z), \qquad (4)$$

where μ is the ground state molecular dipole moment. The Taylor series convention (the so-called T convention) for the theoretically determined values of β was used in this work [51].

Scan over the first-order hyperpolarizability for the central torsional angle was performed for all investigated molecules. The data presented in Figs. 2 and 3 were interpolated using cubic splines method from Gnuplot program [52]. The nonlinear least-squares (NLLS) Marquardt-Levenberg algorithm implemented in the same program was used to calculate parameters A and B (Eq. 1).

Results and discussion

Geometrical structure

As was mentioned in the Introduction, the NLO properties of betaine dyes are strongly affected by conformational parameters. Hence, in this part of the report extended discussion of the results of calculations of the geometrical structures for this class of compounds is presented. In Table 1 the values of the angle ϕ and the C-N and C-O bond distances obtained with the 6–31G(d) basis set at the HF and MP2 levels of theory are presented. The first observation is that the inclusion of electron correlation energy has a strong effect on the geometries of the
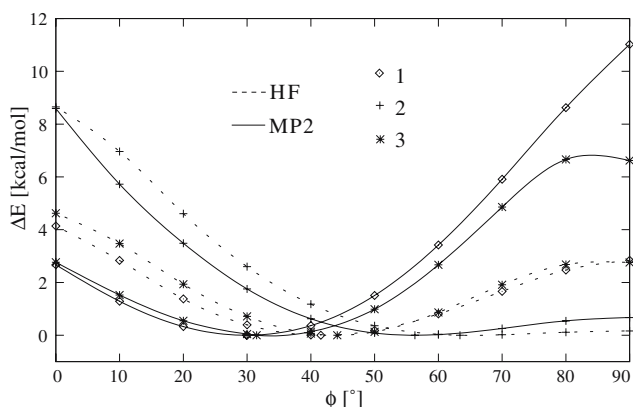

Fig. 2 The energy profiles for central torsional angle (relative to (min (E)) for molecules investigated in the present study obtained at the HF/6–31G(d) and MP2/6–31G(d) levels of theory
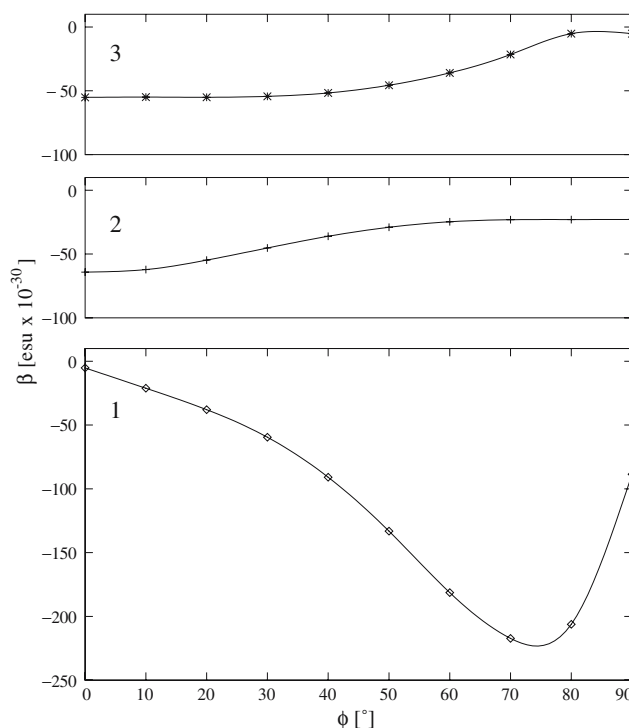

Fig. 3 The scan of the first-order hyperpolarizability for ϕ angle obtained with MP2/6–31+G(d) method at geometries obtained at the MP2/6–31G(d) level of theory

investigated molecules. In comparison to the HF results for all of the investigated molecules, at the MP2 level of theory, the angle ϕ is smaller by approximately 10° and the bond C-O is longer by 0.030 Å. The differences are not so uniform for the C-N bond. The discrepancy between the HF and MP2 results is 0.042 Å for **1** and 0.033 Å for **3**, but only 0.015 Å for betaine dye **2**.

It is clear that there is a strong steric repulsion between *ortho* atoms (the hydrogens atoms in **1**, **2** and the hydrogen and the oxygen atoms in **3**), which makes structures of the investigated molecules non-planar. The ϕ angle is very similar for molecules **1** and **3**. However, the distance between *ortho* atoms is smaller in **3** − 1.99 Å compared to 2.12 Å for isomer **1**. Moreover, the C-O and the C-N bonds are longer in **3** than in **1**. These variations are caused by the different positions of the oxygen atom. However, the differences between **1**, **3** pair and isomer **2** are much larger. The central C-N bond is longer and the ϕ angle larger for **2**

Table 1 Geometrical parameters of investigated molecules (MP2/6–31G(d))

	ϕ [°]		C-N [Å]		C-O [Å]	
	HF	MP2	HF	MP2	HF	MP2
1	41.57	29.91	1.424	1.382	1.219	1.248
2	57.54	48.15	1.468	1.453	1.227	1.257
3	44.14	33.72	1.448	1.415	1.241	1.266

than for **1** and **3**. If we take into account that the interaction between *ortho* atoms has similar character in isomers **1** and **2**, these differences allow to conclude that the conjugation of π systems is weaker in molecule **2** than in other isomers.

It should be noted that there are experimental data only for molecule **1** [53]. It is quite surprising that φ and the C–N bond length obtained without the electron correlation is closer to the experimental data. However, it does not mean that the HF is to overperform MP2 method. The experimental geometry are extracted from crystallographic data, but the present theoretical calculation does not take into account any environmental influences. Ishida and Rossky demonstrated that solvents strongly affected the geometry of **1** [22]. The value of φ is ~6° higher in acetonitrile and water than in the gas phase. The φ angle in water (46.79°) is very close to the data for **1**·2H$_2$O crystal (47.26°), so errors introduced by the lack of electron correlation and the environment effect can cancel each other.

As mentioned in the Introduction, there are no literature reports on molecule **2** and there are only two studies of the optimal geometry parameters of molecule **3** [32, 35]. González et al. reported the geometries obtained with the AM1 Hamiltonian, HF method (6–311G basis set) and Density Functional Theory (B3LYP functional with 6–311G basis set) [32]. This work shows that the effect of the inclusion of the electron correlation is similar to the results of our calculations, i.e. the φ angle becomes smaller, the C-N bond shorter and the C-O bond longer than at non-correlated level. Moreover, the AM1 method gives geometry closer to the methods including electron correlation (B3LYP, MP2) than to the HF method. Similar observations remain valid for the molecule **1** [33]. There are some disagreements between the HF results presented above and those given by González et al. [32]. The most important difference is connected with the length of C-O bond. However, it should be noticed that the quantum chemical calculations presented by González et al. were carried out using basis sets without polarization functions [32].

An important structural aspect of the investigated molecules are torsional barriers and potential energy dependence on the central angle φ [25, 33, 54]. The energy scans obtained at the HF/6–31G(d) and MP2/6–31G(d) levels of theory are shown in Fig. 2. Additionally, in Fig. 2 the values of the energy for the optimal geometries were presented. There are similarities between energy profiles for the molecules **1** and **3**. The HF/6–31G(d) energy curves is essentially the same and for both molecules the calculated torsional barriers are about 4 kcal/mol for 0° and 2 kcal/mol for 90°. The profiles at the MP2 level are also similar. Small angle (0° – 30°) regions of the curves are close to each other, medium angle regions are similar as well. There are only discrepancies for higher angles. The energy profiles for the molecule **3** reach maximum near 80°, what is in agreement with the MP2/6–31G data recently presented by Hernandes et al. [25]. However, the calculated ratio of the torsional barrier heights $[(\Delta E_{90} = E(\phi = 90°) - E(equilibrium))/(\Delta E_0 = E(\phi = 0°) - E(equilibrium))]$ is much larger than unity for both molecules. This ratio as well as the potential energy profile are different for the isomer **2**. The inclusion of electron correlation does not change the shape of energy curve for this molecule. The barrier at 0° is much higher than the barrier at 90°, $\Delta E_{90}/\Delta E_0$ is equal to 0.019 for HF and 0.078 for MP2.

Non-linear optical properties

The static first-order hyperpolarizability was calculated for the ground state geometry obtained at the MP2/6–31G(d) level of theory. The calculated components of the β tensor obtained at the HF and MP2 levels of theory with three basis sets [6–31+G(d), aug-cc-PVDZ and Z3PolX] are presented in Table 2. The values of β_μ calculated according to Eq. 3 are also presented in Table 2. Additionally, the values of β_{xxx} for **1** obtained with eight basis sets are presented in Table 3.

Table 2 Dipole moment (μ [D]) and first-order hyperpolarizability (β [10^{-30} esu]) of investigated molecules

		μ_x		β_{xxx}		β_{xyy}		β_{xzz}		β_μ	
		HF	MP2	HF	MP2	HF	MP2	HF	MP2	HF	MP2
1	6–31+G(d)	14.33	10.82	−127.14	−60.13	3.26	3.38	−0.71	−1.04	−74.75	−34.68
	z3-pol	14.17	10.62	−122.91	−70.38	2.78	3.01	−0.47	−0.77	−72.36	−40.89
	aug-cc-PVDZ	14.05	10.42	−126.21	−57.97	2.94	3.00	−0.52	−0.87	−74.28	−33.50
2	6–31+G(d)	15.27	14.11	−10.91	−30.07	−2.70	−1.92	−0.77	−0.80	−8.87	−19.02
	z3-pol	15.04	13.83	−10.31	−29.32	−2.70	−1.63	−0.67	−0.76	−8.14	−17.59
	aug-cc-PVDZ	15.01	13.76	−10.64	−29.96	−2.31	−1.57	−0.66	−0.71	−8.36	−18.60
3	6–31+G(d)	7.03	5.98	−26.56	−53.60	0.87	0.86	0.45	0.40	−14.64	−29.07
	z3-pol	6.94	5.92	−25.38	−52.09	0.67	0.67	0.41	0.40	−14.04	−28.43
	aug-cc-PVDZ	7.14	6.03	−26.63	−55.04	0.99	1.19	0.49	0.49	−14.38	−29.36

Table 3 First-order hyperpolarizability (β [10^{-30} esu]) of **1** obtained with different basis sets

		HF	MP2
6–31G	135	−107.94	−44.71
6–31G(d)	213	−104.04	−35.25
6–31G(d,p)	240	−104.55	−35.10
6–31+G(d)	265	−127.14	−60.13
6–31++G(d,p)	301	−127.94	−59.37
6–311+G(d)	313	−128.47	−57.46
Z3PolX	288	−122.90	−70.38
aug-cc-PVDZ	380	−126.21	−57.97

The values in the second column correspond to the number of basis function.

The most important observation is connected with the fact that β_μ is dominated by the *xxx* component. The value of β_{xxx} is the smallest for **2**, and the largest for the isomer **1** at all investigated levels of theory. However, β_μ has a negative sign for all investigated molecules. The difference in optical activity of these isomers is probably connected with the character of the low-laying excited state. In the case of the isomer **1** the excited state exhibits more significant CT character in comparison with molecules **2** and **3**.

Additionally, the inclusion of the electron correlation has a different effect on NLO properties of the investigated molecules. It is quite unusual, that the NLO response decreases for molecule **1** upon inclusion of the electron correlation [34]. However, the results of calculations of the first-order hyperpolarizability at the CCSD/6–31+G(d) level ($\beta_{xxx} = -93.67 \times 10^{-30}$ esu) indicates that the correlation effect included at the MP2 level of approximation is overestimated. This observation is in agreement with theoretical benchmark studies for small molecules [55, 56]. It was shown that the CCSD results for electrical properties of the molecular systems are generally of high accuracy.

The opposite effect occurs for isomers **2** and **3**. The longitudinal component of β increases by a factor of three and two, for molecule **2** and **3**, respectively. This is in agreement with the data for *p*-nitroaniline (PNA) which is an typical donor-acceptor π-conjugated system. Sim et al. have shown that the first-order hyperpolarizability obtained using the MP2 method is 88% larger in comparison with the HF method [57].

Fig. 4 Dispersion effect for the investigated molecules obtained at the TDHF/6–31+G(d) level of theory for a) **1** b) **2** and **3** isomers. The geometry of all molecules obtained at the MP2/6–31G(d) level of theory
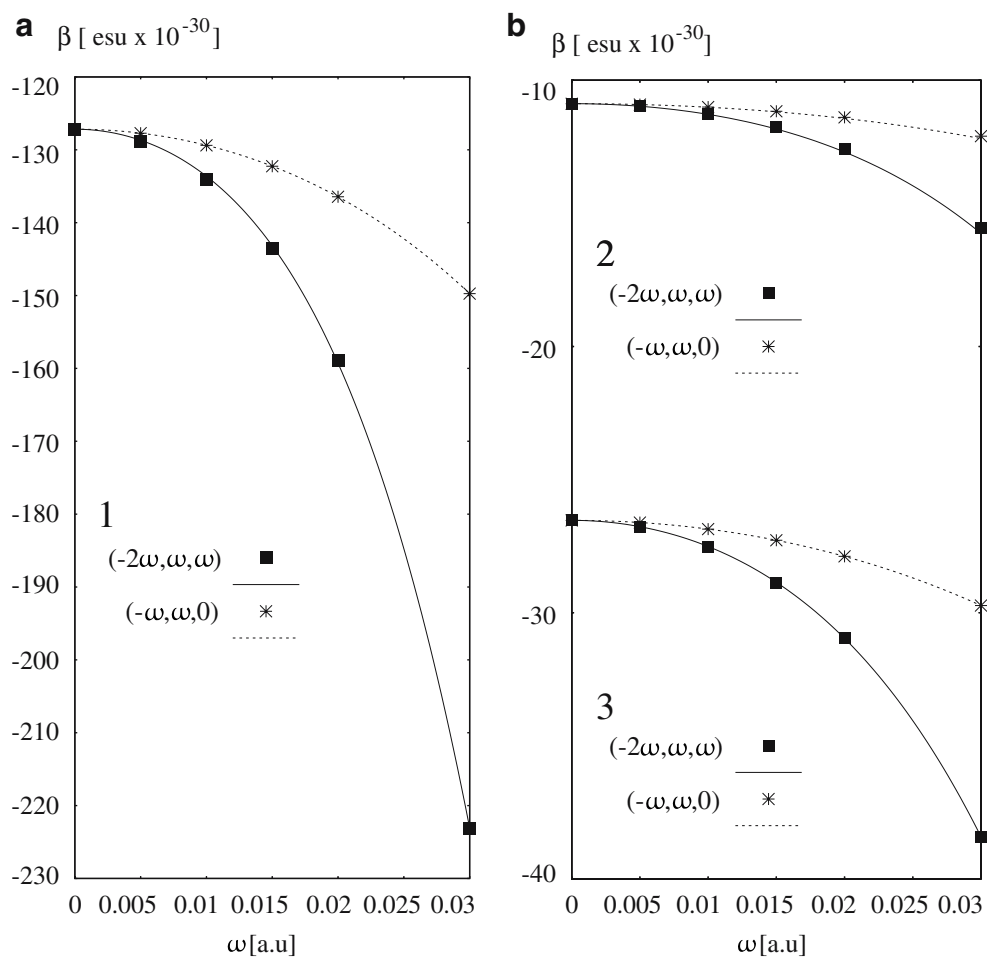
Table 4 Coefficient of the power-series expansion $\beta_{xxx}(\omega_\sigma, \omega_1, \omega_2) = \beta_{xxx}(0,0,0)\left[1 + A\omega_L^2 + B\omega_L^4\right]$ in the 0.00–0.03 frequency range

	$\beta_{xxx}(-2\omega, \omega, \omega)$		$\beta_{xxx}(\omega, 0, 0)$	
	A	B	A	B
1	77.71	11465	85.40	7331
2	53.67	4823	56.93	3035
3	58.99	4437	61.10	3284

Results of our quantum chemical calculation confirm the observation that the inclusion of diffuse functions in basis set is more important for calculation of molecular hyperpolarizability than the polarization functions (see Table 3). Farther extension of basis set size did not significantly change the β_{xxx} value for the molecule **1**. It is important to notice that the Z3PolX basis set give results for β, at the HF level, in very good agreement with the aug-cc-PVDZ basis set. On the other hand, including electron correlation at the MP2 level leads to a 22% overestimation of β_{xxx} in comparison with MP2/aug-cc-PVDZ result. Recently, similar results were found for the absolute value of the first-order hyperpolarizabilities of hydrogen bonded complex [58].

In their review, Kanis et al. classified molecules according to the magnitude of the values of β_μ [4]. All of the molecules investigated here belong to the group of molecules exhibiting large NLO response. However, the comparison of the absolute value of β can be misleading, because the size of the molecule is not taken into account. Therefore, Morley and Pugh suggested that hyperpolarizability density ($\rho = \beta/V_{mol}$ where V_{mol} is molecular volume) should be use to classify molecules [59]. Additionally, a figure-of-merit (FOM) was defined as ratio of β_μ and a molecular weight ($F_0 = \beta_x\mu_g/MW$) [60, 61]. The absolute value of the FOM at the MP2/6–31+G(d) level are equal to 5.39, 4.24 and 3.38 for the **1**, **2** and **3** isomers, respectively. These values are one order larger in comparison to the FOM value of PNA (0.59) [57]. They are also larger than the FOM for Disperse Red 1 (DR1) molecule,

used as a reference molecule by Acebal [61]. Moreover, the FOM for **1** is higher in comparison to the FOM of PMnh2-D - pyrromethene derivative designed to obtained large first-order hyperpolarizability [61]. Another interesting observation is that the FOM is higher for **2** compared to **3**. This is because of a much higher dipole moment of the **2** molecule (see Table 2).

Additionally, the scan over the static first-order hyperpolarizability for the central torsional angle ϕ was performed. The results of these calculations are presented in Fig. 3. It is interesting that the scans for betaines **2** and **3** are quite similar. For both molecules the highest response (absolute value of β_{xxx}) is observed for structure with $\phi=0°$. However, the maximum for molecule **3** is much wider. The results for the optimal geometry ($\phi=34°$) are nearly equal to maximum of the first-order hyperpolarizability for this molecule. The picture of the first-order hyperpolarizability scan is different for **1** isomer. Maximum value of β_{xxx} is 4–5 times higher than in the case of other investigated molecules and it is found for 70°–80°, what is in agreement with the previously presented results [19, 23]. However, there are some differences between these results. The maximal response is 3.6 times higher than the value obtained for the optimal geometry. This ratio is much smaller for the semiempirical GRINDOL/FF [62] results reported previously [19]. Moreover, β_{xxx} does not vanish for the twisted structure and nearly vanishes ($\beta_{xxx} = -5.21 \times 10^{-30}$ esu) for the planar conformer for the MP2 calculations. However, it should be noted that both scans (GRINDOL and MP2) were performed on the different geometries. It was shown previously that there are some discrepancies between the MP2 and AM1 geometry for twisted structure [33]. It should be noticed that the direction of changes of the values of β (for the molecule **1**) as a function of the ϕ angle may be explain in the spirit of the two-level approximation [19, 23]. Another aspect of the NLO response investigated in the present work is the dispersion phenomenon. The frequency dependent first-order hyperpolarizabilities for the second harmonic generation

Table 5 The values of first-order hyperpolarizability (β [10^{-30} esu]) for laser characteristic frequencies

		ω [a.u]	β_{xxx}^{HF}	β_{xxx}^{MP2}	β_μ^{HF}	β_μ^{MP2}
1	$\beta(-2\omega, \omega, \omega)$	0.04282	−654.33	−309.46	−386.39	−179.26
	$\beta(-\omega, \omega, 0)$	0.04282	−181.24	−85.72	−107.19	−49.73
		0.06563	−351.76	−166.39	−209.51	−97.20
2	$\beta(-2\omega, \omega, \omega)$	0.04282	−28.84	−79.49	−17.14	−36.75
	$\beta(-\omega, \omega, 0)$	0.04282	−13.67	−37.68	−10.88	−23.33
		0.06563	−20.69	−57.03	−16.11	−34.55
3	$\beta(-2\omega, \omega, \omega)$	0.04282	−64.27	−129.70	−36.10	−71.68
	$\beta(-\omega, \omega, 0)$	0.04282	−33.77	−68.15	−18.70	−37.13
		0.06563	−50.10	−101.11	−27.94	−55.48

$\beta(-2\omega,\omega,\omega)$ and the optical rectification $\beta(-\omega,\omega,0)$ process presented here were obtained using TDHF method. Low frequency β_{xxx} (0 to 0.03 a.u.) was used to resolve Eq. 1 and to draw a graph of β as a function of ω presented in Fig. 4. Coefficients A and B obtained from fitting Eq. 1, are listed in Table 4. The dispersion effect is much stronger for betaine dye 1 compared to other isomers. For example the ratio of the first-order hyperpolarizability for $\omega =$ 0.03 a.u. to static response $(\beta(0.03)/\beta(0))$ for SHG process is equal to 1.75, 1.43 and 1.45 for the molecule 1, 2 and 3, respectively. Additionally, the values of β for the laser characteristic frequencies are presented in Table 5. Because 2ω is too close to the resonance the results of β_{SHG} for ruby laser frequency are not included.

It has been suggested that the electron correlation effect for frequency dependent properties may be estimated from the ratio of the static correlated values and the TDHF results [50, 63]. Equation 2 was used to obtain the MP2 values of the frequency dependent first-order hyperpolarizability. These values are presented in Table 5. However, it should be noted that this method of evaluation of β_{MP2} has many limitations [64]. One of the most important restrictions for the presented results is that the low-laying electron transition state decreases the reliability of the frequency dependence obtained in this approximation [19, 20, 23, 28, 32, 65].

Conclusions

The quantum chemical calculations of the simplest pyridinium-N-phenolate betaine dye isomers were performed. Comparison of the geometries of the investigated molecules leads to the conclusion that the geometrical structure of the betaine 3 is much closer to 1 than to 2. A similar conclusion can be drawn from analysis of the potential energy curve for the ϕ angle rotation. Moreover, in contrast to isomer 2, the inclusion of electron correlation strongly affects the shape of the energy profile for the central angle ϕ for the molecules 1 and 3. However, the electron correlation changes the geometry of all investigated molecules.

Another issue addressed in this study was the comparison of the first-order hyperpolarizabilities for the investigated betaine dyes. The most important conclusion is that there are significant differences in NLO properties between 1 and other investigated molecules. The inclusion of electron correlation reduces the values of β_{xxx} for molecule 1 but enlarges for 2 and 3. However, the β_{μ} component is dominated by the β_{xxx} for all isomers. Additionally, the value of β of the isomer 1 is much more strongly affected by the change of the ϕ angle. Its maximum value is 4–5 times larger compared to the other investigated molecules and was obtained for the structure with $\phi \sim 70° - 80°$,

whereas the maximum value of β for the other investigated molecules was obtained for planar structure. The dispersion effect is also much stronger for the betaine 1.

The Z3PolX basis set was constructed particularly for calculations of the dipole moment and polarizability. Our results indicated small discrepancies in the case of the estimates of the static, molecular first-order hyperpolarizabilities of the isomer 1. However, it was found that the Z3PolX basis set is generally a reliable choice for the calculations of the NLO properties of large molecular systems.

In the future it would be necessary to explain, in spirit of the multilevel approximations, origin of the very large electron correlation effect on β of the investigated betaine isomers. Our experience indicates that the excited states properties of isomer 1 should be described based on a multireference method. Work on this field is in progress.

References

1. Brèdas JL, Adant C, Tackx P, Persoon A (1994) Chem Rev 94:243–278
2. Nalwa HS, Miyata S (eds) (1997) Nonlinear optics of organic molecules and polymers. CRC, Boca Raton
3. Bishop DM, Norman P (2000) In: Nalwa HS (ed) Nonlinear optical materials, vol 9, ch 1 of Hanbook of Advanced Electronic and Photonic Materials and Devices. Academic, San Diego,
4. Kanis DR, Ratner MA, Marks TJ (1994) Chem Rev 94:195–242
5. Oudar JL, Chemla DS (1977) J Chem Phys 66:2664–2668
6. Reichardt C (1992) Chem Rev Soc (London) 21:147–153
7. Reichardt C (1994) Chem Rev 94:2319–2356
8. Reichardt C (1998) Solvents and solvents effects in orgainc chemistry. VCH, Weinheim
9. Reichardt C (2004) Pure Appl Chem 76:1903–1919
10. Paley MS, Meehan EJ, Smith CD, Rosenberger FE, Howard SC, Harris JM (1989) J Org Chem 54:3432–3436
11. Paley MS, Harris JM (1991) J Org Chem 56:568–574
12. Abe J, Shirai Y (1996) J Am Chem Soc 118:4705–4706
13. Abe J, Shirai Y, Nemoto N, Miyata F, Nagase Y (1997) J Phys Chem B 101:576–582
14. Abe J, Nemoto N, Nagase Y, Shirai Y (1996) Chem Phys Lett 261:18–22
15. Abe J, Shirai Y, Nemoto N, Miyata F, Nagase Y (1997) J Phys Chem B 101:1910–1915
16. Laxmikanth Rao J, Bhanuprakash K (1998) J Mol Struct (THEOCHEM) 458:269–273
17. Sitha S, Laxmikanth Rao J, Bhanuprakash K, Choudary BM (2001) J Phys Chem A 105:8727–8733
18. Sworakowski J, Lipiński J, Ziolek L, Palewska K, Nešpůrek S (1996) J Phys Chem A 100:12288–12294
19. Bartkowiak W, Lipiński J (1998) J Phys Chem A 102:5236–5240
20. Lipiński J, Bartkowiak W (1999) Chem Phys 245:263–276
21. Mente SR, Maroncelli M (1999) J Phys Chem B 103:7704–7718
22. Ishida T, Rossky P (2001) J Phys Chem A 105:558–565

23. Zaleśny R, Bartkowiak W, Styrcz S, Leszczynski J (2002) J Phys Chem A 106:4032–4037
24. Morley JO, Padfield J (2002) J Chem Soc Perkin Trans 2:1698–1707
25. Hernandes MZ, Longo R, Coutinho K, Canuto S (2004) Phys Chem Chem Phys 6:2088–2092
26. Jasien PG, Weber LL (2001) J Mol Struct (THEOCHEM) 572:203–212
27. Hogiu S, Dreyer J, Pfeiffer M, Brzezinka KW, Wencke W (2000) J Raman Spectrosc 31:797–803
28. Fabian J, Rosquete GA, Montero-Cabrera LA (1999) J Mol Struct (THEOCHEM) 469:163–176
29. Lobaugh J, Rossky P (1999) J Phys Chem A 103:9432–9447
30. Hwang H, Rossky P (2004) J Phys Chem A 108:2607–2616
31. Hwang H, Rossky P (2004) J Phys Chem B 108:6723–6732
32. González D, Neilands O, Rezende MC (1999) J Chem Soc Perkin Trans 2:713–717
33. Niewodniczński W, Bartkowiak W, Leszczynski J (2005) J Mol Model 11:392–397
34. Bartkowiak W, Niewodniczński W, Misiaszek T, Zaleśny R (2005) Chem Phys Lett 441:8–13
35. Caricato M, Mennucci B, Tomasi J (2004) J Phys Chem A 108:6248–6256
36. Spassova M, Enchev V (2004) Chem Phys 298:29–36
37. Benkova Z, Sadlej AJ, Oakes RE, Bell SEJ (2005) J Comput Chem 26:145–153
38. Benková Z, Sadlej AJ, Oakes RE, Bell SEJ (2005) Theor Chem Acc 113:238–247
39. Oakes RE, Bell SEJ, Benkova Z, Sadlej AJ (2005) J Comput Chem 26:154–159
40. Zaleśny R, Bartkowiak W (2005) Int J Quantum Chem 104:660–666
41. Benková Z, Černušák I, Zahradník P (2006) Mol Phys 104:2011–2026
42. Frisch MJ, Trucks GW, Schlegel HB, Scuseria GE, Robb MA, Cheeseman JR, Montgomery JA Jr, Vreven T, Kudin KN, Burant JC, Millam JM, Iyengar SS, Tomasi J, Barone V, Mennucci B, Cossi M, Scalmani G, Rega N, Petersson GA, Nakatsuji H, Hada M, Ehara M, Toyota K, Fukuda R, Hasegawa J, Ishida M, Nakajima T, Honda Y, Kitao O, Nakai H, Klene M, Li X, Knox JE, Hratchian HP, Cross JB, Bakken V, Adamo C, Jaramillo J, Gomperts R, Stratmann RE, Yazyev O, Austin AJ, Cammi R, Pomelli C, Ochterski JW, Ayala PY, Morokuma K, Voth GA, Salvador P, Dannenberg J, Zakrzewski V, Dapprich S, Daniels AD, Strain MC, Farkas O, Malick DK, Rabuck AD, Raghavachari K, Foresman JB, Ortiz JV, Cui Q, Baboul AG, Clifford S, Cioslowski J, Stefanov BB, Liu G, Liashenko A, Piskorz P, Komaromi I, Martin RL, Fox DJ, Keith T, Al-Laham MA, Peng CY, Nanayakkara A, Challacombe M, Gill PMW, Johnson B, Chen W, Wong MW, Gonzalez C, Pople JA (2004) Gaussian 03, revision C.02. Gaussian, Inc., Wallingford, CT
43. Schmit MW, Baldridge KK, Boatz JA, Elbert ST, Gordon MS, Jensen JH, Koseki S, Matsunaga N, Nguyen KA, Su SJ, Windus TL, Dupuis M, Montgomery JA (1993) J Comput Chem 14:1347–1463
44. (2005) Dalton, an ab initio electronic structure program, release 2.0
45. Torrent-Sucarrat M, Sol M, Duran M, Luis JM, Kirtman B (2003) J Chem Phys 118:711–718
46. Yang M, Jacquemin D, Champagne B (2002) Phys Chem Chem Phys 4:5566–5571
47. Kurtz H, Dudis D (1998) Review in computational chemistry, vol 12. VCH, New York, p 241
48. Bishop DM (1991) J Chem Phys 95:5489
49. Rice JE, Handy NC (1991) J Chem Phys 94:4959–4971
50. Rice JE, Handy NC (1992) Int J Quantum Chem 43:91–118
51. Willetts A, Rice JE, Burland DM, Shelton DP (1992) J Chem Phys 97:7590–7599
52. Williams T, Kelley C et al (2004) gnuplot 4.0 patchlevel 0
53. Wojtas Ł, Pawlica D, Stadnicka K (2006) J Mol Struct 785:14–20
54. Caricato M, Mennucci B, Tomasi J (2006) Mol Phys 104:875–887
55. Pecul M, Pawłowski F, Jørgensen P, Köhn A, Hättig C (2006) J Chem Phys 124:114101–114111
56. Larsen H, Olsen J, Hättig C, Jørgensen P, Christiansen O, Gauss J (1999) J Chem Phys 111:1917–1925
57. Sim F, Chin S, Dupuis M, Rice JE (1993) J Phys Chem 97:1158–1163
58. Skwara B, Bartkowiak W, Zawada A, Góra RW, Leszczynski J (2007) Chem Phys Lett 436:116–123
59. Morley JO, Pugh D (1989) Spec Publ-R Soc Chem 69:28–39
60. Moylan CR, Swanson SA, Walsh CA, Thackara JI, Twieg RJ, Miller RD, Lee VY (1993) SPIE Proc 2025:192–201
61. Acebal P, Blaya S, Carreto L (2003) Chem Phys Lett 382:489–495
62. Lipiński J (1988) J Int J Quantum Chem 34:423–435
63. Sekino H, Bartlett R (1991) J Chem Phys 94:3665–3669
64. Dalskov EK, Jørgen H, Jensen Å, Oddershede J (1997) Mol Phys 90:3–14
65. Fabian J (2001) Theor Chem Acc 106:199–217